

Review

Not peer-reviewed version

Weight-Bearing CT for Diseases around the Ankle Joint

[Jahyung Kim](#) , [Jaeyoung Kim](#) , [Saintpee Kim](#) , [Young Yi](#) *

Posted Date: 15 July 2024

doi: [10.20944/preprints2024071005.v2](https://doi.org/10.20944/preprints2024071005.v2)

Keywords: Weight-bearing; CT; ankle arthritis; syndesmosis injury; osteochondral lesion of talus; ankle instability



Preprints.org is a free multidiscipline platform providing preprint service that is dedicated to making early versions of research outputs permanently available and citable. Preprints posted at Preprints.org appear in Web of Science, Crossref, Google Scholar, Scilit, Europe PMC.

Copyright: This is an open access article distributed under the Creative Commons Attribution License which permits unrestricted use, distribution, and reproduction in any medium, provided the original work is properly cited.

Disclaimer/Publisher's Note: The statements, opinions, and data contained in all publications are solely those of the individual author(s) and contributor(s) and not of MDPI and/or the editor(s). MDPI and/or the editor(s) disclaim responsibility for any injury to people or property resulting from any ideas, methods, instructions, or products referred to in the content.

Review

Weight-Bearing CT for Diseases around the Ankle Joint

Jahyung Kim ¹, Jaeyoung Kim ², Saintpee Kim ³ and Young Yi ^{4,5,*}

¹ Department of Orthopedic Surgery, Seoul National University Hospital, Seoul National University College of Medicine, Seoul, Korea; hpsyndrome@naver.com

² Baylor University Medical Center, Dallas, Texas, USA; jaeyoungkimj@gmail.com

³ Department of Orthopedic Surgery Gangbuk Etteum hospital, Seoul Korea; ksb8060@gmail.com

⁴ Department of Orthopedic Surgery, Sanggye Paik Hospital, Inje University College of Medicine,

⁵ Department of Orthopaedic Surgery and Rehabilitation, Yale School of Medicine, New Haven, CT, USA

* Correspondence: y.yi@yale.edu; Tel.: 82-2-2270-0236, 1-203-500-4636

Abstract: Weight-bearing computed tomography (WBCT) enables acquisition of three-dimensional bony structure images in a physiological weight-bearing position, which is fundamental in understanding the pathologic lesions and deformities of the ankle joint. Over the past decade, researchers focused on validating and developing WBCT measurements, which has significantly enhanced our knowledge of common foot and ankle disease. Consequently, understanding the application of WBCT in clinical practice is becoming more important to produce improved outcomes in the treatment of disease around the ankle joint. This review will describe an overview of what is currently being evaluated in the foot and ankle surgery using WBCT and where the course of research will be heading in the future.

Keywords: weight-bearing; CT; ankle arthritis; syndesmosis injury; osteochondral lesion of talus; ankle instability

Introduction

Comprehensive understanding of foot and ankle region is often challenging to orthopaedic surgeons due to its highly complicated anatomical and biomechanical structures that are closely interrelated. In addition, it is essential to appreciate their altered position and alignment with weight-bearing to fully address the patient's symptoms during walking or running. In other words, pathologic conditions such as impingement, joint space narrowing, and malalignment may only be apparent with load during assessment, which could be left undiagnosed if evaluated without weight-bearing [1].

Although conventional standing radiographs allow clinicians to identify the ankle in a weight-bearing position, these provide limited information to foot and ankle surgeons owing to its low spatial resolution and overlaps with adjacent bones [2]. To overcome the shortcomings of computed tomography (CT) and magnetic resonance imaging (MRI) which are usually obtained in a supine manner, several attempts have been made to evaluate the foot and ankle pathologies under simulated weight-bearing condition using custom-made loading devices [3,4]. Unfortunately, these devices only enabled partial weight-bearing, which could underestimate the physiologic loading of the ankle joint compared with normal fully weight-bearing position. In addition, such methods could not reflect muscle activation, which plays a significant role in determining the positions of the bones and their relationships with the joints.

Cone-beam CT (CBCT), which was primarily utilized in dental diagnostics, involves the use of a cone-shaped X-ray beam and two-dimensional (2D) detectors that acquire volumetric data with less rotation of the X-ray source compared with conventional CT [2]. Because the detector moves around the patient during CBCT scanning, development of weight-bearing CT (WBCT) became possible and its adoption in foot and ankle area permitted an important technical step forward. It enables

acquisition of bony structure images in a physiological weight-bearing position, which is fundamental to apprehending the degenerative lesions and deformities of the ankle joint. In practice, weight-bearing CBCT combines the advantages of high spatial resolution three-dimensional (3D) imaging with weight-bearing and muscle activation, allowing the exact reproduction of dimensions and proportions. Additional advantages of WBCT include a rapid image acquisition time, a reduced cost, and a low radiation dose [5].

Over more than ten years of its usage in foot and ankle surgery, numerus studies have been executed to better utilize WBCT in clinical practice. Researchers focused on developing and validating the WBCT measurements and provide information that cannot be obtained in conventional methods. Such efforts have significantly enhanced our knowledge of foot and ankle pathologic condition. The purpose of this review article is to introduce radiologic measurements of the WBCT and their ongoing clinical usage in diseases around the ankle joint.

A. Normal anatomy

Since first introduced in foot and ankle surgery, WBCT has been used to investigate normal foot and ankle anatomy in patients without significant pathology. Especially, WBCT has been frequently applied on healthy control patients to discover rotational movements of the talus within the mortise and subtalar joint configuration, which could not be evaluated through weight-bearing plain radiograph due to superimposition of bones [6,7]. Lepojärvi et al investigated the talar movement by measuring the rotation of the talus, medial clear space, anterior and posterior widths of the tibiotalar joint, transition of the talus, and talar tilt in 32 healthy subjects [6]. They concluded that when the ankle is taken from maximal internal to maximal external rotation, the talus rotates a total of 10 degrees internally-externally about the tibia with no substantial widening of the medial clear space. In order to determine the morphology and orientation of posterior facet of the subtalar joint, Collin et al analyzed 59 healthy volunteers without hindfoot and ankle pathologies [7]. They found that the posterior facet was concave in 88% and flat in 12%, while it was oriented valgus in 90% and varus in 10% when measured in the middle coronal plane. Authors added that the posterior facet of the subtalar joint is consistently oriented in valgus, whereas the most anterior aspect of the posterior facet of the subtalar joint is typically oriented in varus. This study suggests that the measurements of the varus-valgus orientation of the posterior facet of the subtalar joint could be dependent on where the CT image is taken in the anterior-posterior direction.

Another study by Ritcher et al combined WBCT with a custom pedography sensor to describe the relative position of the anatomic foot center and the pedographic center of gravity during weight-bearing. Authors analyzed 180 feet in 90 patients and found that the anatomic foot center was distal to the center of gravity of the foot in 97% of feet at a mean distance of 27.5 mm, while it was lateral to the center of gravity in 62% of feet, by a mean of 2.0 mm. This finding suggests that there is a constant major distal longitudinal shift of center of gravity relative to foot center and an inconstant minor mediolateral shift [8].

A. Ankle Osteoarthritis

WBCT offers significant clinical advantages in ankle osteoarthritis (OA) because thinning of the cartilage and manifestation of deformities around the ankle joint become more evident under load [9]. It also better reflects geometric characteristics of the ankle joint and allows for more accurate measurements compared with a conventional radiograph [2]. The WBCT is therefore utilized for precise diagnosis and classification of the pathologic condition, along with detailed establishment of therapeutic strategies.

Diagnosis

The use of WBCT in the diagnosis of ankle OA begins with a stereotaxic understanding of the position of the talus relative to the ankle mortise. The amount of pathologically altered ankle structure may suggest severity of ankle arthritis. Kim et al used talus rotation ratio to quantify abnormal internal rotation of the talus and concluded that the talus is abnormally internally rotated in patients

with varus ankle arthritis [10]. They also added that patients with severe varus ankle osteoarthritis showed a higher incidence of abnormal talus internal rotation compared with those with moderate varus ankle osteoarthritis (Figure 1). Song et al evaluated the amount of correction after SMO using an axial loading CT, which showed significantly corrected abnormal internal rotation of the talus [4]. These findings indicate that not only the coronal and sagittal pathologic components of the ankle OA that can easily be visualized with conventional radiographs, but the axial component which can only be obtained with WBCT should also be considered to evaluate the disease.



Figure 1. Abnormal internal rotation of talus in the axial plane in varus ankle arthritis. Plain weight-bearing anteroposterior ankle radiography of the normal ankle (A-1) with corresponding WBCT axial image showing the congruent position of the talus in the ankle joint, without rotation against the lateral malleolus (LM) (A-2). Plain weight-bearing anteroposterior ankle radiography of a patient with varus ankle osteoarthritis (B-1), with WBCT axial image showing the internally rotated talus against the lateral malleolus (LM) (B-2).

In addition, several studies attempted to diagnose ankle OA by measuring the joint space width (JSW) using WBCT. Wiley et al first applied JSW to evaluate the joint space narrowing in posttraumatic ankle osteoarthritis, which showed good reliability and reproducibility [11]. The measurement was performed in a single-value, 2D manner made at selected locations. With the development of technology, however, software-driven 3D geometric measurements of the distance between bone surfaces became possible (Figure 2) [12]. Although its automated imaging process of the measurements needs to be improved, 3D JSW mapping may enhance intuitive visualization of the ankle joint biomechanics. Furthermore, it provides highly sensitive monitoring of joint space narrowing, which may be used as an alternative indicator for progression in joint disease.



Figure 2. Bounding box method to detect the joint width narrowing using automated intelligence (AI) with the Xelis 3D imaging software (INFINITT Healthcare, Korea).

The hindfoot alignment and compensation of the subtalar joint should also be taken into consideration when making therapeutic strategies for ankle OA. Because the measurements in hindfoot alignment view are known to be sensitive to changes in x-ray beam projection angle, WBCT is particularly useful to evaluate the hindfoot alignment [13,14]. Krähenbühl et al evaluated the subtalar joint orientation using coronal WBCT images and concluded that the subtalar joint was more varus oriented in varus ankle OA while more valgus oriented in valgus ankle OA (Figure 3) [15]. They also studied the degree of inframalleolar compensation against supramalleolar abnormalities with WBCT, stating that subtalar joint compensation occurred in varus ankle OA whereas it did not happen in valgus ankle OA. Similarly, Kang et al focused on subtalar compensation in advanced varus ankle arthritis and found that ankle OA with talar tilt angle greater than 9.5 degrees is significantly prone to a non-compensated heel [16]. Likewise, WBCT is actively being used to explain the hindfoot alignment and subtalar joint characteristics in ankle OA.



Figure 3. Weight-bearing plain radiographs of patients with various types of tibiotalar alignment (A-1, B-1, C-1) and corresponding subtalar joint orientation in WBCT (A-2, B-2, C-2). The subtalar vertical angle (SVA) was defined as the inclination of the line connecting the medial and lateral aspects of the talus with a vertical line, which is perpendicular to the ground.

Classification

The Takakura classification is based on the ankle mortise weight-bearing plain radiograph findings, which is useful when monitoring the progression of arthritis [17]. Although it is probably the most widely used classification worldwide, there are some forms of arthritis that cannot be explained by this system because it solely uses a 2D coronal plane image. Kim et al measured the ratio of medial gutter width to tibial plafond-talar dome space in coronal images of the anterior, middle, and posterior ankle, defining medial gutter narrowing as a ratio less than 0.5 [18]. Interestingly, the anterior part of the ankle joint showed valgus talar tilt rather than varus, contradicting our existing belief that medial gutter arthritis is a feature of a subtype of varus ankle OA described in Takakura classification. Other plain radiographs-based classifications may also be limited to completely reflect the 3D characteristics of ankle OA [19,20].

Using the WBCT, Richter et al proposed a classification, which subdivided ankle OA into four degrees [21]. The first-degree ankle OA includes joint space narrowing, which is not a complete loss, and osteophyte formation (Figure 4A). The second degree includes a partial or total loss of joint space (Figure 4B). The third degree implies presence of additional subchondral cysts with remaining joint surface congruence (Figure 4C). The fourth degree includes additional joint destruction with incongruity of the articular surface (Figure 4D). Authors commented that the new classification may effectively combine the classic features of osteoarthritis (joint space narrowing, osteophyte formation, and subchondral cysts) along with 3D visualization.



Figure 4. A classification system proposed by Richter et al. [21] (A) First degree of osteoarthritis with osteophyte formation and joint space narrowing, but not complete loss (B) Second degree of osteoarthritis with partial or complete loss of joint space. (C) Third degree of osteoarthritis with additional subchondral cysts, with remaining joint surface congruency. (D) Fourth degree of osteoarthritis with aggravated joint surface destruction and incongruence.

Besides, Tazegul et al developed and described a computational method that enables objective quantitative assessment of OA using WBCT image intensity, i.e., Hounsfield units [9]. Authors used four projections at different location throughout the joint and allowed intuitive visualization on which quadrants have reduced joint space width and contrast. Although the study simply proposed a computational methodology with small sample size, quantitative measurements and selection of

objective points within each joint may further improve the reliability and reproducibility of OA classification.

Treatment

a) Deformity correction surgery

Supramalleolar osteotomy (SMO) is an established surgical option to correct valgus or varus deformity in patients presenting with ankle OA [22]. It is a joint preserving modality that is utilized for management of early to mid-stage asymmetric ankle arthritis [23]. The procedure may bring about load shift of the weight-bearing axis, thereby redistributing and decreasing the peak stress concentration within the ankle mortise [24]. WBCT is being used to preoperatively determine the expected amount of correction and to postoperatively evaluate the changes of ankle joint position in 3D manner (Figure 5) [4]. Furthermore, Burssens et al described changes in subtalar joint alignment in sagittal and axial planes after SMO, indicating that WBCT can be used to elucidate the subtalar joint behavior in ankle arthritis that can be ignored in 2D approaches [25].

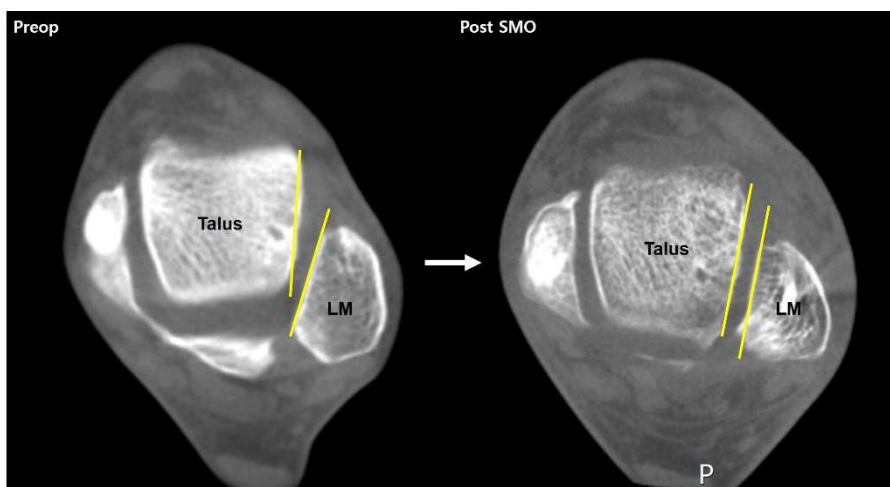


Figure 5. A case of a varus ankle osteoarthritis patient showing correction of abnormal internal rotation of the talus after supramalleolar osteotomy (SMO).

WBCT can also improve the accuracy of corrective osteotomies by assisting development of a patient specific guide. Using the patient specific guide, appropriate level of the osteotomy can be determined based on the fit of the guide and a virtual correction can be performed preoperatively until the desired position is achieved [21]. In their pilot study, Facit et al suggested that a dome-shaped supramalleolar osteotomy using 3D-printed guides designed on WBCT can be used to potentially mitigate the technical drawbacks of free-hand osteotomies [26].

b) Ankle replacement surgery

Total ankle arthroplasty (TAA) has emerged as a viable option for end stage ankle OA [27]. It has gained significant popularity within the last decades among foot and ankle surgeons with drastically increasing usage rates [28–31]. Such an increasing trend for using this procedure might be due to some of its advantages compared with ankle arthrodesis: the ability to preserve ankle joint motion, to provide a more physiologic gait, and to minimize the risk of adjacent joint arthritis [32–34]. With technical improvements in implant design and surgical technique, multiple studies have proven that TAA can provide equivocal or better clinical outcomes than ankle arthrodesis [35,36].

In order to produce satisfactory outcomes and minimize failure, implants must be properly placed within the ankle joint [37]. In this sense, WBCT based patient-specific instrumentation guides make accurate bony resection based on patient's anatomy possible in TAA. Because there is no intraoperative navigation system for TAA currently available, integrating WBCT into the preoperative planning process enables determination of potential implant size and positions, which would allow for less variability in the operating room [38].

Preoperative WBCT may also be utilized in determining the adjunctive procedures to be performed along with TAA. de Cesar Netto et al utilized preoperative WBCT generated foot and ankle offset (FAO) to retrospectively review the number of corrective bony realignment procedures performed at the time of TAA [39]. They concluded that the number of additional osseous realignment procedures significantly correlated with preoperative FAO, with valgus malalignment patients requiring a greater number compared with varus patients. The finding can be implied that preoperative FAO can predict the number of bony realignment procedures necessary for TAA, which may eventually enhance the preoperative assessment and surgical planning for patients undergoing TAA.

Although TAA is now indicated as an appropriate treatment modality for end stage ankle OA, complications following the joint replacement surgery are still reported in the literature with considerable incidence rates. A recent systematic analysis reviewed 22 studies which included 4412 ankles from 4276 patients who underwent TAA, with mean follow-up of 66.6 ± 40.9 months [40]. The review reported an adjusted mean complication rate of 23.7% (2.4-52%), mostly high-grade complications (35.6%) such as deep infection, aseptic loosening, or implant failure [41].

The most common complications known to contribute to revision surgery after TAA are deep infection, aseptic loosening, and implant subsidence [33,42]. With this regard, WBCT can be an effective postoperative diagnostic option to detect early implant failure or periprosthetic cyst formation (Figure 6). Lintz et al found out that 81% of 60 patients who underwent TAA had periprosthetic cysts in WBCT at a mean follow-up of 44.6 months [43]. They also demonstrated threshold values of FAO for patients with residual malalignment following TAR, where values below -2.75% in varus cases and above 4.5% FAO in valgus cases could predict increased risks of periprosthetic cyst formation. Considering these findings, it seems reasonable to recommend WBCT scan for complete 3D assessment of the alignment and early detection of complications in patients who underwent TAR.

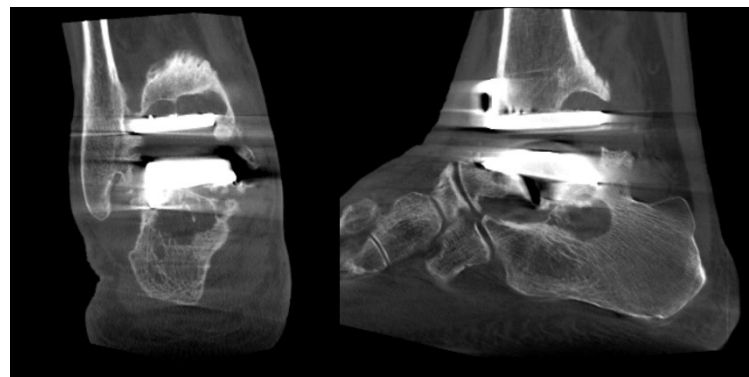


Figure 6. Multiple periprosthetic cysts can be detected using WBCT.

B. Syndesmosis injury

Ignored or inadequately treated syndesmosis injury could result in significant long-term morbidity including pain, instability, and degenerative changes of the ankle joint [44]. Unfortunately, precise diagnosis of syndesmotic injuries remains difficult, especially if the injury is subtle. In fact, diagnosis of syndesmosis injury has been relied on various imaging modalities, which have inherent limitations. First, inability of conventional CT or MRI to evaluate the syndesmotic structures under load or stress limits their reliability. Second, establishing the normal range indicating abnormal radiographic measurement in syndesmosis injury is challenging because of significant anatomic variation among individuals. For this reason, experts recommend using the unaffected contralateral ankle as a reference to determine the abnormality of the syndesmosis [45,46].

WBCT is being acknowledged as a useful diagnostic tool owing to its ability to directly assess the biomechanics of the tibiofibular joint under physiologic load. In addition, simultaneous visualization of the contralateral ankle under equivalent physiologic load makes the WBCT imaging

more beneficial in evaluating the syndesmotic injuries. In accordance with such advantages, several studies have focused on diagnostic applications of the WBCT in syndesmotic injuries [47].

Recently, instead of relying on the linear or angular measurements, multiple studies introduced dimensional or volumetric assessment using the WBCT, which was shown to be accurate in estimating syndesmotic injury. Hagemeijer et al described the circumferential area measurement using WBCT and found that patients with unilateral syndesmotic instability showed significantly increased syndesmotic area of the injured side compared with contralateral uninjured side [48]. To better induce syndesmotic widening, studies have demonstrated addition of external rotation torque during WBCT measurements and confirmed better diagnostic accuracy [49,50]. With this regard, Shamrock et al reported normal threshold values of syndesmotic area measurements [51]. Over 50 uninjured ankles who underwent WBCT scans with external rotation stress on their ankle, axial-plane WBCT images measured on 1cm proximal to the apex of the tibial plafond showed the mean syndesmotic area of $106.7 \pm 18.3 \text{ mm}^2$. Beyond this 2D area measurement, advanced measurement modalities like volumetric measurement would allow for improved diagnostic efficiency for syndesmotic in the future (Figure 7) [52].

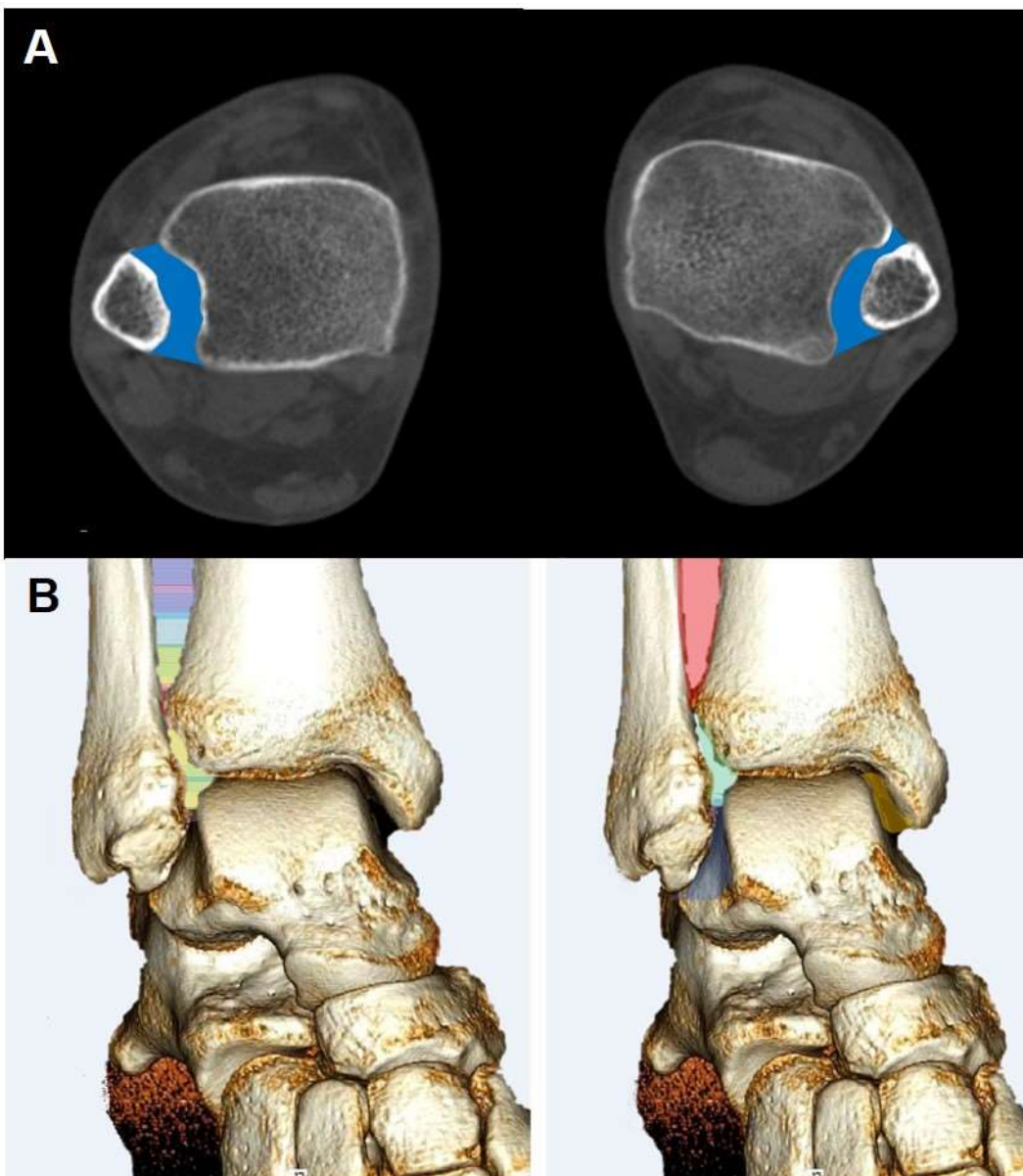


Figure 7. Methods to estimate the syndesmosis injury. A. circumferential area measurement B. volumetric measurement.

C. Osteochondral lesion of talus

Keys to successful therapeutic outcomes for osteochondral lesion of talus (OLT) may depend on the surgeon's ability to optimize adequate surgical intervention to the lesion. As a result, it is critical to precisely measure the lesion's surface, volume, and depth during preoperative planning in OLT surgery. Conventional imaging modalities like CT or MRI, however, are known to over- or underestimate the lesion's measurements [53,54]. Alternatively, distance mapping (DM), which is a new imaging modality that provides quantitative visualization of the joint surface distance distribution on each articular bone, may propose some possibility for more accurate evaluation of the lesion's dimension in OLT when used with WBCT (Figure 8) [55,56]. In other words, intuitive assessment of the OLT is possible because DM can demonstrate the distance between bones in the form of color-coded maps.



Figure 8. Illustration showing distance mapping analysis using Xelis 3D imaging software (INFINITT Healthcare, Korea).

Efrima et al measured the surface, depth, and volume of 40 OLTs using WBCT and DM and estimated the reliability of a renewed imaging modality [57]. The interclass correlation of the measurements using the devices showed excellent inter-rater and intra-rater agreement. Subsequently, when asked to choose the therapeutic options based on the measurement, evaluators achieved a near-perfect agreement on preferred surgical approach. Although further studies would be needed to support their findings, introduction of WBCT along with DM in OLT surgery may hold significant implications to enhance agreement for preoperative planning.

D. Chronic ankle instability

Compared with other disease entities around the ankle joint, literature regarding the use of WBCT in chronic ankle instability (CAI) is limited. Previous studies focused on correlation between bony alignment and CAI. Van Bergeyk et al compared hindfoot alignment of 12 patients with CAI with 12 control patients using simulated WBCT and found that measurements indicating calcaneal varus deformity showed 3 to 4 degrees more varus in the CAI patients than the control patients [58]. Researchers concluded that hindfoot varus alignment was a significant risk factor contributing to recurrent ankle instability. Lintz et al confirmed the finding in their comparative study of 34 patients with CAI and 155 patients without ankle instability [59]. They found a 35% increased odds ratio of CAI per 1% increase in varus hindfoot alignment.

In their narrative review, Lintz et al proposed possible usages of dynamic WBCT imaging to better explore CAI [60]. They described that traditional varus and anterior drawer dynamic imaging

of the bilateral ankle is possible with WBCT, which may provide vast amount of information that cannot be obtained from the conventional dynamic radiographs. First, automatic axes calculation or simultaneous associated fracture detection can be possible with semiautomatic segmentation (Figure 9). Second, with the use of DM, objective assessment of tibiotalar tilt would be available because it offers intuitive colorized map along with precise numeric quantification of the distance between articular surfaces in a defined area. Finally, utilization of supplementary devices like customized jigs to provoke stress can minimize some of the downsides of dynamic imaging: poor reproducibility and increased motion artifacts.



Figure 9. Semi-automatic segmentation of the bones around the ankle joint using Xelis 3D imaging software (INFINITT Healthcare, Korea).

E. Acute ankle sprain

Following acute ankle sprain, multiple views, such as oblique or lateral views, are often required in a conventional radiographic setup to detect lesions that are not clearly visible owing to bone superimposition. Furthermore, there is a belief that radiographs in acute ankle sprain should not be performed in a standing manner because weight-bearing would provoke pain or deformation of the injured limb in the context of trauma. Consequently, additional conventional CT is often administered for patients with suspected bony lesions, which will eventually result in high radiation-exposure and time consumption for patients.

In fact, WBCT does not have to be taken with patient standing. While the term “weight-bearing” was named because of its historical appeal to the surgeons, most available products provide a mobile device to enable patients to remain seated during the examination (Figure 10). Moreover, digitally reconstructed radiographs (DRR) can now be created and implemented using WBCT (Figure 11)[61]. As a result, surgeons confronting acute ankle sprains may benefit from an all-in-one radiographic modality that could offer delicate spatial resolution of 0.27 to 0.35mm for enhanced diagnosis, without causing pain or discomfort to injured patients. Jacques et al executed a prospective comparative study on 165 emergency patients who underwent the classical 2D x-ray-multi-detector CT pathway versus 224 patients for which CBCT was used as a primary imaging modality [62]. They reported a 35% reduction in radiation dose and a 15% reduction in turnover time. In summary, WBCT can effectively be used in acute ankle sprain to reduce the number of false-negatives or delayed diagnosis of concomitant pathology, radiation exposure, time to diagnosis, time spent in the emergency department, and direct and secondary costs [60].



Figure 10. Most of the commercially available WBCTs provide a mobile device to enable patients to remain seated during the examination.



Figure 11. A digitally reconstructed radiograph (DRR) anteroposterior view of the ankle joint.

Conclusion

Over the course of a decade, WBCT has changed the understanding of pathologic condition around the ankle joint and is currently being used to revolutionize the therapeutic consequences. Moreover, there is still a vast opportunity for future research on the impact of WBCT in terms of clinical decision-making and practical usage. In fact, WBCT is yet to be globally used because there are a lot more to be improved such as limitation in automatic measurement or necessity of specialized software or professionals for 3D analysis [63,64]. Nevertheless, we believe that technological improvement will somehow enable foot and ankle surgeons to overcome the shortcomings and to further employ WBCT as a standard diagnostic imaging tool for disorders of the ankle joint.

References

1. Barg, A.; Bailey, T.; Richter, M.; de Cesar Netto, C.; Lintz, F.; Burssens, A.; Phisitkul, P.; Hanrahan, C.J.; Saltzman, C.L. Weightbearing Computed Tomography of the Foot and Ankle: Emerging Technology Topical Review. *Foot Ankle Int* **2018**, *39*, 376-386, doi:10.1177/1071100717740330.

2. Lintz, F.; de Cesar Netto, C.; Barg, A.; Burssens, A.; Richter, M. Weight-bearing cone beam CT scans in the foot and ankle. *EFORT Open Rev* **2018**, *3*, 278-286, doi:10.1302/2058-5241.3.170066.
3. Kang, D.H.; Kang, C.; Hwang, D.S.; Song, J.H.; Song, S.H. The value of axial loading three dimensional (3D) CT as a substitute for full weightbearing (standing) 3D CT: Comparison of reproducibility according to degree of load. *Foot Ankle Surg* **2019**, *25*, 215-220, doi:10.1016/j.fas.2017.10.014.
4. Song, J.H.; Kang, C.; Kim, T.G.; Lee, G.S.; Lee, J.K.; Ahn, K.J.; Kim, D.H.; Lee, S.W. Perioperative axial loading computed tomography findings in varus ankle osteoarthritis: Effect of supramalleolar osteotomy on abnormal internal rotation of the talus. *Foot Ankle Surg* **2021**, *27*, 217-223, doi:10.1016/j.fas.2020.04.006.
5. Richter, M.; Lintz, F.; de Cesar Netto, C.; Barg, A.; Burssens, A. Results of more than 11,000 scans with weightbearing CT - Impact on costs, radiation exposure, and procedure time. *Foot Ankle Surg* **2020**, *26*, 518-522, doi:10.1016/j.fas.2019.05.019.
6. Lepojärvi, S.; Niinimäki, J.; Pakarinen, H.; Koskela, L.; Leskelä, H.V. Rotational Dynamics of the Talus in a Normal Tibiotalar Joint as Shown by Weight-Bearing Computed Tomography. *J Bone Joint Surg Am* **2016**, *98*, 568-575, doi:10.2106/jbjs.15.00470.
7. Colin, F.; Horn Lang, T.; Zwicky, L.; Hintermann, B.; Knupp, M. Subtalar joint configuration on weightbearing CT scan. *Foot Ankle Int* **2014**, *35*, 1057-1062, doi:10.1177/1071100714540890.
8. Richter, M.; Lintz, F.; Zech, S.; Meissner, S.A. Combination of PedCAT Weightbearing CT With Pedography Assessment of the Relationship Between Anatomy-Based Foot Center and Force/Pressure-Based Center of Gravity. *Foot Ankle Int* **2018**, *39*, 361-368, doi:10.1177/1071100717744206.
9. Tazegul, T.E.; Anderson, D.D.; Barbachan Mansur, N.S.; Kajimura Chinelati, R.M.; Iehl, C.; VandeLune, C.; Ahrenholz, S.; Lalevee, M.; de Cesar Netto, C. An Objective Computational Method to Quantify Ankle Osteoarthritis From Low-Dose Weightbearing Computed Tomography. *Foot Ankle Orthop* **2022**, *7*, 24730114221116805, doi:10.1177/24730114221116805.
10. Kim, J.B.; Yi, Y.; Kim, J.Y.; Cho, J.H.; Kwon, M.S.; Choi, S.H.; Lee, W.C. Weight-bearing computed tomography findings in varus ankle osteoarthritis: abnormal internal rotation of the talus in the axial plane. *Skeletal Radiol* **2017**, *46*, 1071-1080, doi:10.1007/s00256-017-2655-0.
11. Willey, M.C.; Compton, J.T.; Marsh, J.L.; Kleweno, C.P.; Agel, J.; Scott, E.J.; Bui, G.; Davison, J.; Anderson, D.D. Weight-Bearing CT Scan After Tibial Pilon Fracture Demonstrates Significant Early Joint-Space Narrowing. *J Bone Joint Surg Am* **2020**, *102*, 796-803, doi:10.2106/jbjs.19.00816.
12. Turmezei, T.D.; Malhotra, K.; MacKay, J.W.; Gee, A.H.; Treece, G.M.; Poole, K.E.S.; Welck, M.J. 3-D joint space mapping at the ankle from weight-bearing CT: reproducibility, repeatability, and challenges for standardisation. *Eur Radiol* **2023**, *33*, 8333-8342, doi:10.1007/s00330-023-09718-6.
13. Barg, A.; Amendola, R.L.; Henninger, H.B.; Kapron, A.L.; Saltzman, C.L.; Anderson, A.E. Influence of Ankle Position and Radiographic Projection Angle on Measurement of Supramalleolar Alignment on the Anteroposterior and Hindfoot Alignment Views. *Foot Ankle Int* **2015**, *36*, 1352-1361, doi:10.1177/1071100715591091.
14. Bernasconi, A.; Cooper, L.; Lyle, S.; Patel, S.; Cullen, N.; Singh, D.; Welck, M. Intraobserver and interobserver reliability of cone beam weightbearing semi-automatic three-dimensional measurements in symptomatic pes cavovarus. *Foot Ankle Surg* **2020**, *26*, 564-572, doi:10.1016/j.fas.2019.07.005.
15. Krähenbühl, N.; Tschuck, M.; Bolliger, L.; Hintermann, B.; Knupp, M. Orientation of the Subtalar Joint: Measurement and Reliability Using Weightbearing CT Scans. *Foot Ankle Int* **2016**, *37*, 109-114, doi:10.1177/1071100715600823.
16. Kang, H.W.; Kim, D.Y.; Park, G.Y.; Lee, D.O.; Lee, D.Y. Coronal plane Calcaneal-Talar Orientation in Varus Ankle Osteoarthritis. *Foot Ankle Int* **2022**, *43*, 928-936, doi:10.1177/10711007221088566.
17. TAKAKURA, Y. The Treatment for Osteoarthritis of Ankle Joint. *Japanese Journal of Rheumatism and Joint Surgery* **1986**, *5*, 347-352.
18. Kim, J.B.; Park, C.H.; Ahn, J.Y.; Kim, J.; Lee, W.C. Characteristics of medial gutter arthritis on weightbearing CT and plain radiograph. *Skeletal Radiol* **2021**, *50*, 1575-1583, doi:10.1007/s00256-020-03688-2.
19. Holzer, N.; Salvo, D.; Marijnissen, A.C.; Vincken, K.L.; Ahmad, A.C.; Serra, E.; Hoffmeyer, P.; Stern, R.; Lübbeke, A.; Assal, M. Radiographic evaluation of posttraumatic osteoarthritis of the ankle: the Kellgren-Lawrence scale is reliable and correlates with clinical symptoms. *Osteoarthritis Cartilage* **2015**, *23*, 363-369, doi:10.1016/j.joca.2014.11.010.
20. Krause, F.G.; Di Silvestro, M.; Penner, M.J.; Wing, K.J.; Glazebrook, M.A.; Daniels, T.R.; Lau, J.T.; Stothers, K.; Younger, A.S. Inter- and intraobserver reliability of the COFAS end-stage ankle arthritis classification system. *Foot Ankle Int* **2010**, *31*, 103-108, doi:10.3113/fai.2010.0103.
21. Richter, M.; de Cesar Netto, C.; Lintz, F.; Barg, A.; Burssens, A.; Ellis, S. The Assessment of Ankle Osteoarthritis with Weight-Bearing Computed Tomography. *Foot Ankle Clin* **2022**, *27*, 13-36, doi:10.1016/j.fcl.2021.11.001.
22. Hintermann, B.; Knupp, M.; Barg, A. Supramalleolar Osteotomies for the Treatment of Ankle Arthritis. *J Am Acad Orthop Surg* **2016**, *24*, 424-432, doi:10.5435/jaaos-d-12-00124.

23. Butler, J.J.; Azam, M.T.; Weiss, M.B.; Kennedy, J.G.; Walls, R.J. Supramalleolar osteotomy for the treatment of ankle osteoarthritis leads to favourable outcomes and low complication rates at mid-term follow-up: a systematic review. *Knee Surg Sports Traumatol Arthrosc* **2023**, *31*, 701-715, doi:10.1007/s00167-022-07144-7.
24. Knupp, M.; Stufkens, S.A.; van Bergen, C.J.; Blankevoort, L.; Bolliger, L.; van Dijk, C.N.; Hintermann, B. Effect of supramalleolar varus and valgus deformities on the tibiotalar joint: a cadaveric study. *Foot Ankle Int* **2011**, *32*, 609-615, doi:10.3113/fai.2011.0609.
25. Burssens, A.; Susdorf, R.; Krähenbühl, N.; Peterhans, U.; Ruiz, R.; Barg, A.; Hintermann, B. Supramalleolar Osteotomy for Ankle Varus Deformity Alters Subtalar Joint Alignment. *Foot Ankle Int* **2022**, *43*, 1194-1203, doi:10.1177/10711007221108097.
26. Faict, S.; Burssens, A.; Van Oevelen, A.; Maeckelbergh, L.; Mertens, P.; Buedts, K. Correction of ankle varus deformity using patient-specific dome-shaped osteotomy guides designed on weight-bearing CT: a pilot study. *Arch Orthop Trauma Surg* **2023**, *143*, 791-799, doi:10.1007/s00402-021-04164-9.
27. Lee, G.W.; Wang, S.H.; Lee, K.B. Comparison of Intermediate to Long-Term Outcomes of Total Ankle Arthroplasty in Ankles with Preoperative Varus, Valgus, and Neutral Alignment. *J Bone Joint Surg Am* **2018**, *100*, 835-842, doi:10.2106/jbjs.17.00703.
28. Pugely, A.J.; Lu, X.; Amendola, A.; Callaghan, J.J.; Martin, C.T.; Cram, P. Trends in the use of total ankle replacement and ankle arthrodesis in the United States Medicare population. *Foot Ankle Int* **2014**, *35*, 207-215, doi:10.1177/1071100713511606.
29. Yasutomi, M.; An, V.V.G.; Xu, J.; Wines, A.; Sivakumar, B.S.; Symes, M.J. Trends in the use of ankle arthrodesis and total ankle replacements in Australia over the past 20 years. *Eur J Orthop Surg Traumatol* **2024**, *34*, 1997-2001, doi:10.1007/s00590-024-03884-z.
30. Tapaninaho, K.; Ponkilainen, V.T.; Haapasalo, H.; Mattila, V.M.; Huttunen, T.T.; Repo, J.P. Incidence of ankle arthrodesis and total ankle replacement between 1997 and 2018: A nationwide registry study in Finland. *Foot Ankle Surg* **2023**, *29*, 288-292, doi:10.1016/j.fas.2023.02.014.
31. Tucker, W.A.; Barnds, B.L.; Morris, B.L.; Tarakemeh, A.; Mullen, S.; Schroepel, J.P.; Vopat, B.G. Nationwide Analysis of Total Ankle Replacement and Ankle Arthrodesis in Medicare Patients: Trends, Complications, and Cost. *Foot Ankle Spec* **2022**, *15*, 201-208, doi:10.1177/1938640020950181.
32. Thomas, R.H.; Daniels, T.R. Ankle arthritis. *J Bone Joint Surg Am* **2003**, *85*, 923-936, doi:10.2106/00004623-200305000-00026.
33. Cody, E.A.; Scott, D.J.; Easley, M.E. Total Ankle Arthroplasty: A Critical Analysis Review. *JBJS Rev* **2018**, *6*, e8, doi:10.2106/jbjs.Rvw.17.00182.
34. SooHoo, N.F.; Zingmond, D.S.; Ko, C.Y. Comparison of reoperation rates following ankle arthrodesis and total ankle arthroplasty. *J Bone Joint Surg Am* **2007**, *89*, 2143-2149, doi:10.2106/jbjs.F.01611.
35. Goldberg, A.J.; Chowdhury, K.; Bordea, E.; Hauptmannova, I.; Blackstone, J.; Brooking, D.; Deane, E.L.; Bendall, S.; Bing, A.; Blundell, C.; et al. Total Ankle Replacement Versus Arthrodesis for End-Stage Ankle Osteoarthritis: A Randomized Controlled Trial. *Ann Intern Med* **2022**, *175*, 1648-1657, doi:10.7326/m22-2058.
36. Rodriguez-Merchan, E.C.; Moracia-Ochagavia, I. Results of Total Ankle Arthroplasty Versus Ankle Arthrodesis. *Foot Ankle Clin* **2024**, *29*, 27-52, doi:10.1016/j.fcl.2023.08.010.
37. Thompson, M.J.; Consul, D.; Umbel, B.D.; Berlet, G.C. Accuracy of Weightbearing CT Scans for Patient-Specific Instrumentation in Total Ankle Arthroplasty. *Foot Ankle Orthop* **2021**, *6*, 24730114211061493, doi:10.1177/24730114211061493.
38. Zeitlin, J.; Henry, J.; Ellis, S. Preoperative Guidance With Weight-Bearing Computed Tomography and Patient-Specific Instrumentation in Foot and Ankle Surgery. *Hss j* **2021**, *17*, 326-332, doi:10.1177/15563316211026325.
39. de Cesar Netto, C.; Day, J.; Godoy-Santos, A.L.; Roney, A.; Barbachan Mansur, N.S.; Lintz, F.; Ellis, S.J.; Demetracopoulos, C.A. The use of three-dimensional biometric Foot and Ankle Offset to predict additional realignment procedures in total ankle replacement. *Foot Ankle Surg* **2022**, *28*, 1029-1034, doi:10.1016/j.fas.2022.02.007.
40. Vale, C.; Almeida, J.F.; Pereira, B.; Andrade, R.; Espregueira-Mendes, J.; Gomes, T.M.; Oliva, X.M. Complications after total ankle arthroplasty- A systematic review. *Foot Ankle Surg* **2023**, *29*, 32-38, doi:10.1016/j.fas.2022.09.010.
41. Glazebrook, M.A.; Arsenault, K.; Dunbar, M. Evidence-based classification of complications in total ankle arthroplasty. *Foot Ankle Int* **2009**, *30*, 945-949, doi:10.3113/fai.2009.0945.
42. Lawton, C.D.; Prescott, A.; Butler, B.A.; Awender, J.F.; Selley, R.S.; Dekker Li, R.G.; Balderama, E.S.; Kadakia, A.R. Modern total ankle arthroplasty versus ankle arthrodesis: A systematic review and meta-analysis. *Orthop Rev (Pavia)* **2020**, *12*, 8279, doi:10.4081/or.2020.8279.
43. Lintz, F.; Mast, J.; Bernasconi, A.; Mehdi, N.; de Cesar Netto, C.; Fernando, C.; Buedts, K. 3D, Weightbearing Topographical Study of Periprosthetic Cysts and Alignment in Total Ankle Replacement. *Foot Ankle Int* **2020**, *41*, 1-9, doi:10.1177/1071100719891411.

44. Chun, D.I.; Kim, J.; Kim, Y.S.; Cho, J.H.; Won, S.H.; Park, S.Y.; Yi, Y. Relationship between fracture morphology of lateral malleolus and syndesmotic stability after supination-external rotation type ankle fractures. *Injury* **2019**, *50*, 1382-1387, doi:10.1016/j.injury.2019.05.020.

45. Dikos, G.D.; Heisler, J.; Choplis, R.H.; Weber, T.G. Normal tibiofibular relationships at the syndesmosis on axial CT imaging. *J Orthop Trauma* **2012**, *26*, 433-438, doi:10.1097/BOT.0b013e3182535f30.

46. Kim, J.; Park, J.H.; Kwon, H.W.; Lee, M.; Kim, D.; Choi, Y.J.; Park, K.R.; Lee, S.; Cho, J. Normal Distal Tibiofibular Syndesmosis Assessment Using Postmortem Computed Tomography (PMCT). *Diagnostics (Basel)* **2023**, *14*, doi:10.3390/diagnostics14010036.

47. Li, J.; Fang, M.; Van Oevelen, A.; Peiffer, M.; Audenaert, E.; Burssens, A. Diagnostic applications and benefits of weightbearing CT in the foot and ankle: A systematic review of clinical studies. *Foot Ankle Surg* **2024**, *30*, 7-20, doi:10.1016/j.fas.2023.09.001.

48. Hagemeijer, N.C.; Chang, S.H.; Abdelaziz, M.E.; Casey, J.C.; Waryasz, G.R.; Guss, D.; DiGiovanni, C.W. Range of Normal and Abnormal Syndesmotic Measurements Using Weightbearing CT. *Foot Ankle Int* **2019**, *40*, 1430-1437, doi:10.1177/1071100719866831.

49. Krähenbühl, N.; Bailey, T.L.; Weinberg, M.W.; Davidson, N.P.; Hintermann, B.; Presson, A.P.; Allen, C.M.; Henninger, H.B.; Saltzman, C.L.; Barg, A. Is load application necessary when using computed tomography scans to diagnose syndesmotic injuries? A cadaver study. *Foot Ankle Surg* **2020**, *26*, 198-204, doi:10.1016/j.fas.2019.02.002.

50. Krähenbühl, N.; Bailey, T.L.; Weinberg, M.W.; Davidson, N.P.; Hintermann, B.; Presson, A.P.; Allen, C.M.; Henninger, H.B.; Saltzman, C.L.; Barg, A. Impact of Torque on Assessment of Syndesmotic Injuries Using Weightbearing Computed Tomography Scans. *Foot Ankle Int* **2019**, *40*, 710-719, doi:10.1177/1071100719829720.

51. Shamrock, A.; Den Hartog, T.J.; Dowley, K.; Day, J.; Barbachan Mansur, N.S.; Carvalho, K.A.M.; de Cesar Netto, C.; O'Malley, M. Normal Values for Distal Tibiofibular Syndesmotic Space With and Without Subject-Driven External Rotation Stress. *Foot Ankle Int* **2024**, *45*, 80-85, doi:10.1177/10711007231205576.

52. Bhimani, R.; Ashkani-Esfahani, S.; Lubberts, B.; Guss, D.; Hagemeijer, N.C.; Waryasz, G.; DiGiovanni, C.W. Utility of Volumetric Measurement via Weight-Bearing Computed Tomography Scan to Diagnose Syndesmotic Instability. *Foot Ankle Int* **2020**, *41*, 859-865, doi:10.1177/1071100720917682.

53. Walley, K.C.; Gonzalez, T.A.; Callahan, R.; Fairfull, A.; Roush, E.; Saloky, K.L.; Juliano, P.J.; Lewis, G.S.; Aynardi, M.C. The Role of 3D Reconstruction True-Volume Analysis in Osteochondral Lesions of the Talus: A Case Series. *Foot Ankle Int* **2018**, *39*, 1113-1119, doi:10.1177/1071100718771834.

54. Yasui, Y.; Hannon, C.P.; Fraser, E.J.; Ackermann, J.; Boakye, L.; Ross, K.A.; Duke, G.L.; Shimozono, Y.; Kennedy, J.G. Lesion Size Measured on MRI Does Not Accurately Reflect Arthroscopic Measurement in Talar Osteochondral Lesions. *Orthop J Sports Med* **2019**, *7*, 2325967118825261, doi:10.1177/2325967118825261.

55. Siegler, S.; Konow, T.; Belvedere, C.; Ensini, A.; Kulkarni, R.; Leardini, A. Analysis of surface-to-surface distance mapping during three-dimensional motion at the ankle and subtalar joints. *J Biomech* **2018**, *76*, 204-211, doi:10.1016/j.jbiomech.2018.05.026.

56. Dibbern, K.N.; Li, S.; Vytcharenko, V.; Auch, E.; Lintz, F.; Ellis, S.J.; Femino, J.E.; de Cesar Netto, C. Three-Dimensional Distance and Coverage Maps in the Assessment of Peritalar Subluxation in Progressive Collapsing Foot Deformity. *Foot Ankle Int* **2021**, *42*, 757-767, doi:10.1177/1071100720983227.

57. Efrima, B.; Dahmen, J.; Barbero, A.; Benady, A.; Maccario, C.; Indino, C.; Kerkhoffs, G.; Usuelli, F.G. Enhancing precision in osteochondral lesions of the talus measurements and improving agreement in surgical decision-making using weight-bearing computed tomography and distance mapping. *Knee Surg Sports Traumatol Arthrosc* **2024**, doi:10.1002/kss.12172.

58. Van Bergeyk, A.B.; Younger, A.; Carson, B. CT analysis of hindfoot alignment in chronic lateral ankle instability. *Foot Ankle Int* **2002**, *23*, 37-42, doi:10.1177/107110070202300107.

59. Lintz, F.; Bernasconi, A.; Baschet, L.; Fernando, C.; Mehdi, N.; de Cesar Netto, C. Relationship Between Chronic Lateral Ankle Instability and Hindfoot Varus Using Weight-Bearing Cone Beam Computed Tomography. *Foot Ankle Int* **2019**, *40*, 1175-1181, doi:10.1177/1071100719858309.

60. Lintz, F.; Bernasconi, A.; Ferkel, E.I. Can Weight-Bearing Computed Tomography Be a Game-Changer in the Assessment of Ankle Sprain and Ankle Instability? *Foot Ankle Clin* **2023**, *28*, 283-295, doi:10.1016/j.facl.2023.01.003.

61. Fuller, R.M.; Kim, J.; An, T.W.; Rajan, L.; Cororaton, A.D.; Kumar, P.; Deland, J.T.; Ellis, S.J. Assessment of Flatfoot Deformity Using Digitally Reconstructed Radiographs: Reliability and Comparison to Conventional Radiographs. *Foot Ankle Int* **2022**, *43*, 983-993, doi:10.1177/10711007221089260.

62. Jacques, T.; Morel, V.; Dartus, J.; Badr, S.; Demondion, X.; Cotten, A. Impact of introducing extremity cone-beam CT in an emergency radiology department: A population-based study. *Orthop Traumatol Surg Res* **2021**, *107*, 102834, doi:10.1016/j.otsr.2021.102834.

63. Richter, M.; Schilke, R.; Duerr, F.; Zech, S.; Andreas Meissner, S.; Naef, I. Automatic software-based 3D-angular measurement for Weight-Bearing CT (WBCT) provides different angles than measurement by hand. *Foot Ankle Surg* **2022**, *28*, 863-871, doi:10.1016/j.fas.2021.11.010.
64. Richter, M.; Zech, S.; Naef, I.; Duerr, F.; Schilke, R. Automatic software-based 3D-angular measurement for weight-bearing CT (WBCT) is valid. *Foot Ankle Surg* **2024**, doi:10.1016/j.fas.2024.02.016.

Disclaimer/Publisher's Note: The statements, opinions and data contained in all publications are solely those of the individual author(s) and contributor(s) and not of MDPI and/or the editor(s). MDPI and/or the editor(s) disclaim responsibility for any injury to people or property resulting from any ideas, methods, instructions or products referred to in the content.